

# Genetic interactions of separase regulatory subunits reveal the diverged *Drosophila* Cenp-C homolog

Sebastian Heeger,<sup>1</sup> Oliver Leismann,<sup>1,2</sup> Ralf Schittenhelm, Oliver Schraidt, Stefan Heidmann, and Christian F. Lehner<sup>3</sup>

Department of Genetics, BZMB, University of Bayreuth, 95440 Bayreuth, Germany

**Faithful transmission of genetic information during mitotic divisions depends on bipolar attachment of sister kinetochores to the mitotic spindle and on complete resolution of sister-chromatid cohesion immediately before the metaphase-to-anaphase transition. Separase is thought to be responsible for sister-chromatid separation, but its regulation is not completely understood. Therefore, we have screened for genetic loci that modify the aberrant phenotypes caused by overexpression of the regulatory separase complex subunits Pimples/securin and Three rows in *Drosophila*. An interacting gene was found to encode a constitutive centromere protein. Characterization of its centromere localization domain revealed the presence of a diverged CENPC motif. While direct evidence for an involvement of this *Drosophila* Cenp-C homolog in separase activation at centromeres could not be obtained, in vivo imaging clearly demonstrated that it is required for normal attachment of kinetochores to the spindle.**

[*Keywords:* Centromere; Cenp-A; Cenp-C; kinetochore; separase]

Supplemental material is available at <http://www.genesdev.org>.

Received April 22, 2005; revised version accepted June 29, 2005.

Separase functions as a protease at the metaphase-to-anaphase transition of mitosis (for review, see Nasmyth 2002). At this crucial cell cycle transition, separase cleaves the  $\alpha$ -kleisin subunit (Scc1/Mcd1/Rad21) of the cohesin complex and thereby promotes the final release of sister-chromatid cohesion. The careful control of separase activity during the cell division cycle involves regulatory subunits. Securin is a subunit that accumulates and associates with separase during interphase. It acts as an inhibitor of separase activity. Thus, the rapid degradation of securin at the metaphase-to-anaphase transition via the anaphase-promoting complex/cyclosome (APC/C) pathway of ubiquitin-dependent proteolysis results in separase activation. In *Drosophila*, securin is encoded by the *pimples* (*pim*) gene (Leismann et al. 2000) and the catalytic protease subunit by the *Separase* (*Sse*) gene (Jäger et al. 2001). *Drosophila* *Sse* lacks the extensive N-terminal regulatory domain that is present in separases outside the dipterans because the corresponding gene region appears to have evolved into an independent gene, *three rows* (*thr*) (Herzig et al. 2002; Jäger et al. 2004). *Drosophila* *Thr* binds to *Sse* and is required for

sister-chromatid separation during mitosis (Jäger et al. 2001).

The precise role of *Thr* and the corresponding N-terminal domains in nondipteran separases is not understood. Moreover, *Pim* and other securins are not just separase inhibitors but also contribute in an unknown positive manner to sister-chromatid separation. In fission yeast, securin recruits separase to the mitotic spindle, and similar observations have been described in other organisms (Funabiki et al. 1996; Ciosk et al. 1998; Kumada et al. 1998; Jensen et al. 2001; Herzig et al. 2002; Chestukhin et al. 2003). Separase activation and transport on spindle microtubules might confine its action to the congressed chromosomes in metaphase plates and in particular to the pericentromeric region. This hypothetical scenario might explain why only a minute and preferentially pericentromeric pool of Scc1 appears to be cleaved by separase during mitosis of higher eukaryotic cells, while the large majority of Scc1 remains intact.

To identify additional genes that might contribute to separase regulation and function, we have screened for chromosomal regions that act as genetic modifiers of the aberrant phenotypes resulting from overexpression of *Pim* or a dominant-negative *Thr* fragment during *Drosophila* eye development. Molecular characterization of an interacting locus revealed that it encodes a constitutive centromere protein. Mapping of its centromere localization domain in combination with sequence com-

<sup>1</sup>These authors contributed equally to this work.

<sup>2</sup>Present address: Laboratory of Chromosome and Cell Biology, Rockefeller University, 1230 York Avenue, New York, NY 10021, USA.

<sup>3</sup>Corresponding author.

E-MAIL [chle@uni-bayreuth.de](mailto:chle@uni-bayreuth.de); FAX 49-921-55-2710.

Article and publication are at <http://www.genesdev.org/cgi/doi/10.1101/gad.347805>.

parisons among Drosophilid orthologs allowed its identification as the most diverged Cenp-C homolog. Cenp-C was originally identified as a human autoantigen localized to centromeres (Earnshaw and Rothfield 1985; Saitoh et al. 1992) and found to display limited sequence similarity to budding yeast Mif2 (Brown 1995; Meluh and Koshland 1995), which was identified by mutations affecting the fidelity of chromosome transmission during mitosis (Meeks-Wagner et al. 1986). Homologs have also been described in nematodes (HCP-4) and plants (Dawe et al. 1999; Moore and Roth 2001; Oegema et al. 2001; Shibata and Murata 2004; Talbert et al. 2004). For simplicity, we use Cenp-C as a designation for all these homologs. Interestingly, recent analyses have demonstrated that Cenp-C, as well as Cenp-A, a histone H3 variant present in centromeric nucleosomes, evolve rapidly and adaptively in many lineages, perhaps driven by the rapid evolution of centromeric satellite sequences, and in *Drosophila*, Cenp-C was supposed to be absent (Talbert et al. 2004). Apart from providing further support for the striking sequence divergence of ubiquitous eukaryotic centromere components, our findings also raise the possibility that separase activity might be enhanced by such components.

## Results

### Mutations in Cenp-C modify phenotypic consequences resulting from separase dysregulation

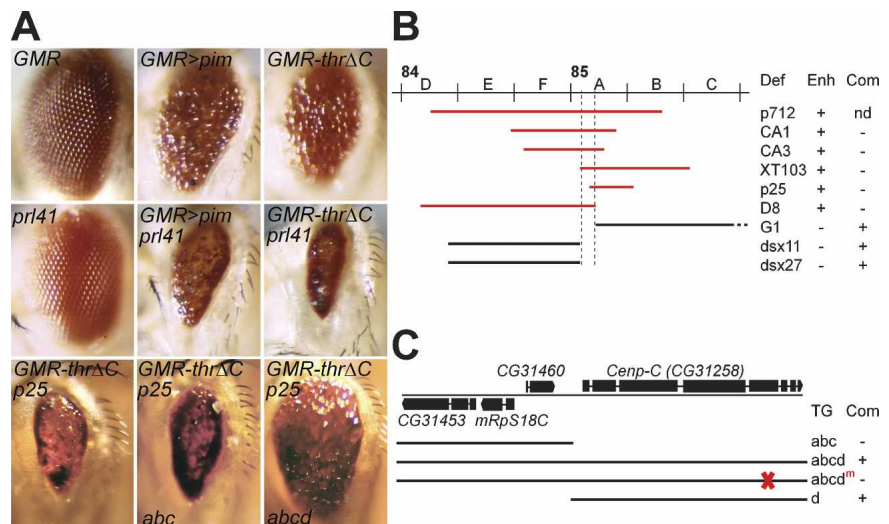
Overexpression of *pim* during *Drosophila* eye development results in an aberrant rough eye phenotype in adults (Fig. 1A, *GMR > pim*). Although we have not characterized this phenotype at a cellular level, we assume

that it results primarily from inhibition of sister-chromatid separation during mitotic divisions of eye imaginal disc cells, because *pim* overexpression during embryogenesis is known to have this effect (Leismann et al. 2000). Moreover, analyses in salivary glands indicated that *pim* overexpression does not have obvious effects in cells progressing through endoreduplication cycles that lack mitotic divisions (data not shown).

When expressed during eye development, a mutant *thr* version lacking C-terminal sequences (*thrΔC*) resulted in a phenotype very similar to that caused by eye-specific *pim* overexpression (Fig. 1A, *GMR-thrΔC*). The effect of *thrΔC* was suppressed by concomitant expression of wild-type *thr*, suggesting that *thrΔC* acts in a dominant-negative manner. The severity of the aberrant phenotypes resulting from *pim* and *thrΔC* overexpression during eye development was correlated with transgene copy numbers (data not shown).

To identify loci interacting with *pim* and *thr*, we crossed a collection of chromosomal deficiencies into the backgrounds with the transgenes resulting in *pim* or *thrΔC* overexpression during eye development. Heterozygosity for the deficiency *Df(3R)p-XT103*, which deletes the chromosomal interval 85A–85C, was found to enhance the rough eye phenotypes caused by *pim* and *thrΔC* overexpression. Based on analyses with additional deficiencies, the interacting region could be narrowed down (Fig. 1B). Moreover, heterozygosity for the EMS-induced, recessive lethal mutation *l(3)85A<sup>prl41</sup>*, which had previously been mapped to this chromosomal region (Jones and Rawls 1988), was also found to enhance the aberrant eye phenotype resulting from *pim* and *thrΔC* overexpression (Fig. 1A, *GMRpim prl41* and *GMR-thrΔC*

**Figure 1.** Separase regulatory subunits encoded by *pim* and *thr* interact genetically with *Cenp-C*. (A) Overexpression of *pim* and C-terminally truncated *thr* during eye development results in an aberrant eye phenotype that is enhanced by mutations in *Cenp-C*. The eyes shown are from flies with the following genotypes: *GMR-GAL4/+ (GMR)*, *GMR-GAL4 UAS-pim-myc II.3/+ (GMR > pim)*, *GMR-thrΔC III.1/+ (GMR-thrΔC)*, *Cenp-C<sup>prl41</sup>/+ (prl41)*, *GMR-GAL4 UAS-pim-myc II.3/+; Cenp-C<sup>prl41</sup>/+ (GMR > pim prl41)*, *GMR-thrΔC III.1/Cenp-C<sup>prl41</sup> (GMR-thrΔC prl41)*, *GMR-thrΔC III.1/Df(3R)p25 (GMR-thrΔC p25)*, *abc II.1/+; GMR-thrΔC III.1/Df(3R)p25 (GMR-thrΔC p25 abc)*, *abcd II.2/+; GMR-thrΔC III.1/Df(3R)p25 (GMR-thrΔC p25 abcd)*. *Df(3R)p25* deletes *Cenp-C* (see panel B), and the transgene insertions *abc* II.1 and *abcd* II.2 carry genomic fragments without and with *Cenp-C*, respectively (see panel C). The latter but not the former transgene reverses the enhancement that *Df(3R)p25* contributes to the phenotype induced by *GMR-thrΔC* III.1. (B) Red lines indicate the chromosomal regions deleted by deficiencies (Def) that scored as enhancers (Enh, +) of the aberrant eye phenotype resulting from overexpression of *pim* or *thrΔC* and that failed to complement *Cenp-C<sup>prl41</sup>* (Com, -), while black lines represent deficiencies with the opposite behavior (Enh, -, Com, +). A locus interacting with *pim* and *thr* is therefore located between the vertical dashed lines. (nd) Not done. (C) Black lines indicate the chromosomal regions and the annotated genes (*CG31453*, *mRpS18C*, *CG31460*, *Cenp-C*) present in transgenes (TG) that were assayed in complementation tests (Com) for their ability to prevent the recessive lethality resulting from *Cenp-C<sup>prl41</sup>* hemizygosity. The frameshift mutation introduced in the *Cenp-C* region of transgene *abcd<sup>tm</sup>* is indicated by the red X.



*prl41*). Complementation tests with *l(3)85Aa<sup>prl41</sup>* and deficiencies breaking within 85A–85C revealed non-complementation in case of deficiencies that enhanced the *pim* and *thrΔC* overexpression phenotype and, conversely, complementation for deficiencies that did not modify this phenotype (Fig. 1B). After molecular mapping of selected deficiency breakpoints, a series of transgenic strains carrying genomic DNA fragments with some of the genes predicted within the identified chromosomal region was generated and used for complementation tests with *l(3)85Aa<sup>prl41</sup>*. Only DNA fragments containing the intact gene *CG31258* were found to prevent the developmental lethality of *l(3)85Aa<sup>prl41</sup>* hemi- and homozygotes (Fig. 1C). Moreover, these fragments also suppressed the enhancing effect of heterozygosity for *l(3)85Aa<sup>prl41</sup>* or noncomplementing deficiencies on the aberrant phenotype caused by *pim* and *thrΔC* overexpression during eye development (Fig. 1A; data not shown). In addition, molecular analyses of the *CG31258* sequence isolated from the *l(3)85Aa<sup>prl41</sup>* chromosome revealed the presence of a premature stop codon instead of a glutamine codon at position 1107 of the predicted protein. Therefore, we conclude that *l(3)85Aa<sup>prl41</sup>* represents a mutant allele of *CG31258* that interacts genetically with *pim* and *thr*.

Furthermore, in a screen for recessive lethals resulting in cell cycle progression defects during embryogenesis, another mutation was subsequently identified that was characterized by a similar embryonic mutant phenotype and map location (K. Dej and T. Orr-Weaver, pers. comm.) and eventually was found to be allelic to *l(3)85Aa<sup>prl41</sup>*. This second allele *l(3)85Aa<sup>IR35</sup>* enhanced the rough eye phenotype resulting from *pim* and *thrΔC* overexpression to the same extent as *l(3)85Aa<sup>prl41</sup>*, and its recessive lethality was also fully complemented by *CG31258* transgenes (data not shown). Sequence analysis of *l(3)85Aa<sup>IR35</sup>* revealed a premature stop codon instead of the glutamine codon at position 858 of the predicted *CG31258* protein.

The most recent gene model of *CG31258* annotated by the *Drosophila* Genome Project agrees with our independent cDNA sequence analyses except for the position of the intron–exon junction at the start of exon 4. Initial database searches with the predicted amino acid sequence did not reveal statistically significant similarities to other genes until sequence traces of various *Drosophilid* genome projects were deposited in the public domain. The sequence comparisons with these *Drosophilid* orthologs in combination with the results of our functional characterizations described below eventually allowed an identification of *CG31258* as the *Drosophila* Cenp-C homolog. In the following, therefore, we designate this gene as *Cenp-C*, even though its identity was recognized only after and because of our functional characterization.

#### Identification of a centromere localization domain in *Cenp-C*

To evaluate the intracellular localization of *Drosophila* Cenp-C, we produced transgenic lines expressing

Cenp-C variants fused either to the enhanced yellow fluorescent protein (EYFP) or to myc epitope copies at the N or C terminus. In addition, affinity-purified rabbit antibodies were generated. Both immunolabeling of wild-type Cenp-C or tagged variants as well as in vivo imaging of EYFP fusions in *Drosophila* embryos (Fig. 2A,D) indicated that Cenp-C is a constitutive centromere protein. This notion was confirmed by comparing the localization of Cenp-C with that of the centromere protein Cid, the *Drosophila* Cenp-A homolog. The comparison revealed colocalization during interphase (Fig. 2D) and mitosis (data not shown).

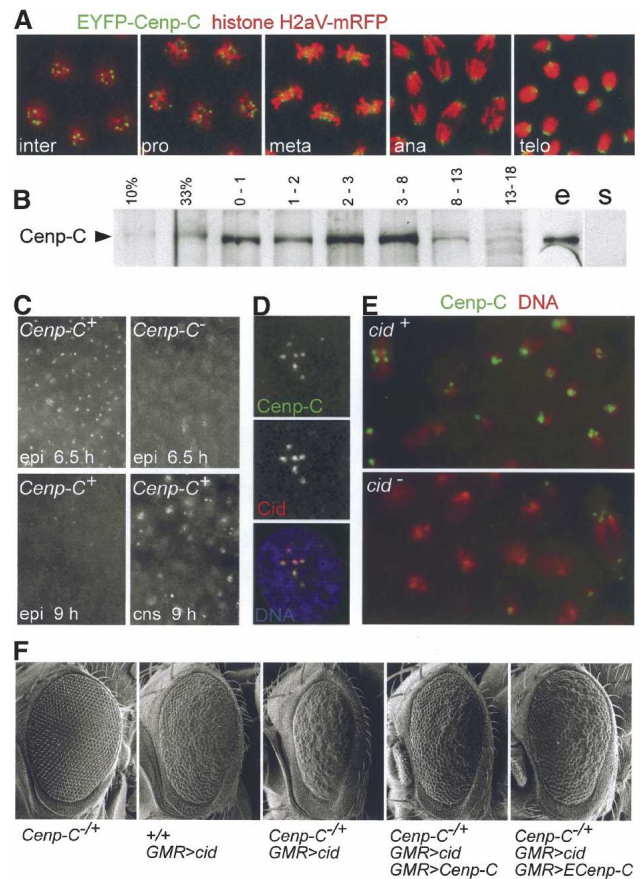
Analysis of Cenp-C expression during development by immunoblotting (Fig. 2B) and immunofluorescence (Fig. 2C) revealed a correlation with mitotic proliferation. Anti-Cenp-C signals declined rapidly in the embryonic epidermis after the final mitotic division, while they were still intense in central nervous system cells that proliferate mitotically. In late embryos, where mitotic proliferation is restricted to only very few cells mainly in the brain, Cenp-C levels were found to be minimal. Moreover, neither immunoblotting (Fig. 2B) nor immunofluorescence and EYFP-Cenp-C fluorescence (data not shown) revealed Cenp-C in the endoreduplicating salivary glands from third instar larvae.

Consistent with the shared intracellular localization of Cid/Cenp-A and Cenp-C, we observed genetic interactions between *cid* and *Cenp-C*. The aberrant rough eye phenotype caused by *cid* overexpression during eye development (Jäger et al. 2005) was found to be enhanced by lowering the number of functional *Cenp-C* gene copies from two to one (Fig. 2F). A noncentromeric excess of overexpressed Cid/Cenp-A, therefore, might titrate limiting amounts of Cenp-C away from the centromere.

Consistent with the idea that Cid/Cenp-A and Cenp-C are in close association, immunolabeling of *cid* mutant embryos with antibodies against Cenp-C revealed that Cid/Cenp-A is required for normal centromeric Cenp-C localization. In *cid* mutant embryos, the presence of a maternal contribution prevents mitotic abnormalities until late in embryogenesis. However, already at earlier developmental stages when maternally contributed Cid/Cenp-A was still detectable (data not shown) and mitotic defects were not yet apparent, anti-Cenp-C signals were clearly weaker in *cid* mutants compared with sibling control embryos (Fig. 2E). Immunolabeling of *Cenp-C* mutant or deficient embryos with anti-Cid/Cenp-A did not reveal a reciprocal dependence of Cid/Cenp-A localization on normal Cenp-C expression and function (see below).

To define centromere localization domains in Cenp-C, we expressed various Cenp-C fragments fused to enhanced green fluorescent protein (EGFP) in *Drosophila* embryos from appropriate transgenes (Fig. 3A). The N-terminal third of Cenp-C (amino acids 1–575) and the central third (amino acids 558–1038) failed to localize the fused EGFP to the centromere (Fig. 3B, N+ and M+). In contrast, the C-terminal third (amino acids 1009–1411) was sufficient to direct efficient centromere localization (Fig. 3B, C+). Further analysis of this region

**Figure 2.** *Drosophila* Cenp-C is a constitutive centromere protein colocalizing and interacting with Cid/Cenp-A. (A) In vivo imaging of syncytial embryos, which express EYFP-Cenp-C (green) and histone H2Av-mRFP (red), indicates that Cenp-C is centromeric during interphase (inter), prophase (pro), metaphase (meta), anaphase (ana), and telophase (telo). (B) Immunoblotting with embryo extracts prepared at different developmental ages (0–1, 1–2, 2–3, 3–8, 8–13, and 13–18 h after egg deposition) revealed high levels of Cenp-C during stages with intense mitotic cell proliferation (0–8 h) and decreasing levels during late embryogenesis when few cells proliferate mitotically (8–18 h). Thirty embryos were loaded per lane except in the first two where three (10%) and 10 (33%) 0–1-h embryos were loaded. Moreover, while Cenp-C was clearly detected in an extract prepared from 20 6–8-h embryos (e), it could not be detected in a comparable amount of protein in an extract prepared from 30 salivary glands of third instar larvae (s). (C) Immunofluorescence experiments with embryos homozygous for *Df(3R)Exel6149*, which deletes *Cenp-C* (*Cenp-C*<sup>-</sup>), and sibling control embryos (*Cenp-C*<sup>+</sup>) revealed strong anti-Cenp-C signals in the epidermis of *Cenp-C*<sup>+</sup> embryos at the stage of mitosis 16 (epi 6.5 h) and in the central nervous system, where mitotic proliferation occurs also at 9 h (cns 9 h). In contrast, weak signals were observed in the post-mitotic epidermis of *Cenp-C*<sup>-</sup> embryos at 9 h (epi 9 h) and already at the stage of mitosis 16 in *Cenp-C*<sup>-</sup> embryos (epi 6.5). (D) An interphase nucleus from a syncytial embryo expressing Cenp-C-myc is shown at high magnification after labeling with anti-myc (top panel and green in bottom panel), anti-Cid/Cenp-A (middle panel and red in bottom panel), and a DNA stain (blue in bottom panel). (E) Labeling of *cid* mutant embryos (*cid*<sup>-</sup>) and sibling control embryos (*cid*<sup>+</sup>) with anti-Cenp-C (green) and a DNA stain (red) indicates that Cid/Cenp-A is required for normal Cenp-C localization at the centromere. High-magnification views of epidermal regions at the stage of mitosis 16 show reduced centromeric anti-Cenp-C signals in *cid* mutants. (F) Overexpression of *cid/Cenp-A* results in an aberrant eye phenotype that is enhanced by mutations in *Cenp-C*. The eyes shown are from flies with the following genotypes: *Cenp-C*<sup>IR35/+</sup> (*Cenp-C*<sup>-/+</sup>), *GMR-GAL4 UAS-cid* II.3B/+ (+/+ *GMR > cid*), *GMR-GAL4 UAS-cid* II.3B/+, *Cenp-C*<sup>IR35/+</sup> (*Cenp-C*<sup>-/+</sup> *GMR > cid*), *GMR-GAL4 UAS-cid* II.3B/*UAS-Cenp-C* II.1; *Cenp-C*<sup>IR35/+</sup> (*Cenp-C*<sup>-/+</sup> *GMR > cid* *GMR > Cenp-C*), *GMR-GAL4 UAS-cid* II.3B/+; *Cenp-C*<sup>IR35/UAS-EGFP-Cenp-C III.2 (*Cenp-C*<sup>-/+</sup> *GMR > cid* *GMR > ECenp-C*).</sup>



indicated that the subregion from amino acids 1009–1205 was also sufficient to confer centromere localization (Fig. 3B, CN+), while two other subregions (amino acids 1094–1306 and 1204–1411) were not sufficient (Fig. 3B, CM+ and CC+).

To identify amino acid positions crucial for centromere localization, we randomly mutagenized the sequences encoding the region sufficient for centromere localization in vitro by error-prone PCR and used these mutated sequences to replace the corresponding wild-type sequence in a construct allowing expression of the C-terminal third of Cenp-C fused to EGFP. Three-hundred-ninety-four mutagenized clones were analyzed for their ability to localize to the centromere after transfection of *Drosophila* SR+ cultured cells. All 50 mutants that had lost centromere localization were subjected to DNA sequence analysis. In addition, 25 randomly selected mutants that localized to the centromere were sequenced as well. These sequences revealed that mutant constructs contained on average 1.9 mutations and that every amino acid position within the region sufficient for centromere binding should have been covered by about two missense mutations in our mutagenesis

experiment. Yet only a single-point mutation (R1101G) that abolished centromere localization in the transfection assay was identified (Fig. 3C,D). R1101, therefore, appears to be of special importance for centromere localization. All other mutants that failed to localize to the centromere were characterized by the presence of premature stop codons. The location of these stop codons in combination with the location of a premature stop codon (1192stop) that did not abolish centromere localization in the transfection assay indicated that the region between amino acids 1084 and 1192 is important for centromere localization (Fig. 3C,D).

#### *Drosophilid Cenp-C homologs contain a diverged CENPC motif*

The deposition of *Drosophilid* genome sequences in the public internet domain allowed the identification of *Cenp-C* orthologs from *Drosophila simulans*, *Drosophila yakuba*, *Drosophila erecta*, *Drosophila ananassae*, *Drosophila pseudoobscura*, and *Drosophila virilis*. Amino acid comparisons between the predicted proteins revealed the presence of conserved blocks (Fig. 4A). Sev-



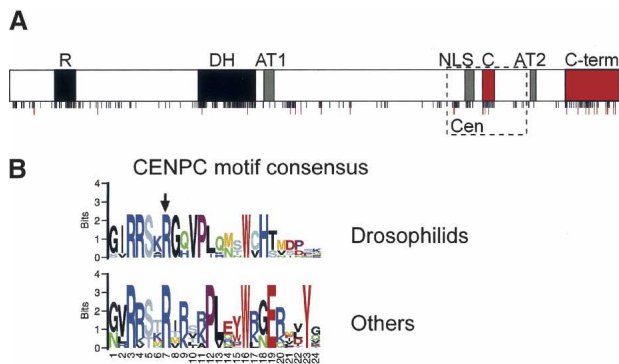


**Figure 4.** Comparison of Cenp-C from *Drosophila* and other metazoans. (A) Identical positions present in an alignment of the amino acid sequences of Cenp-C from *D. melanogaster*, *D. pseudoobscura*, and *D. virilis* are indicated by black lines. Positions that are also identical in an alignment including Cenp-C from *Homo sapiens*, *Mus musculus*, and *Rattus norvegicus* in addition to the three *Drosophila* species are indicated by red lines. The boxes indicating the CENPC motif (C) and the C-terminal region (C-term), which appear to be conserved in all metazoans, are filled in red. The arginine-rich region (R) and another region (DH) that were found to be maximally conserved among *Drosophila* species are illustrated by black boxes. Gray boxes indicate the poorly conserved predicted AT hooks (AT1 and AT2) and nuclear localization signal (NLS). The region sufficient for centromere localization is indicated by a dashed rectangle (Cen). (B) A CENPC motif consensus sequence was derived from the predicted Cenp-C proteins of seven *Drosophila* species (*D. ananassae*, *D. erecta*, *D. melanogaster*, *D. pseudoobscura*, *D. simulans*, *D. virilis*, *D. yakuba*) and found to deviate from the consensus sequence derived from fungal, plant, and other metazoan Cenp-C proteins (Talbert et al. 2004), in particular toward the C-terminal end.

ing this region (deletion of amino acids 36–546) fail to localize to the centromere (Fig. 3A; data not shown).

Three other small regions of *D. melanogaster* Cenp-C displayed similarities to nuclear localization signals (amino acids 1058–1075) (Fig. 3A, NLS) and to AT hooks, which can mediate binding to the minor groove of DNA (amino acids 593–612 and amino acids 1207–1219) (Fig. 3A, AT1 and AT2). These regions showed limited conservation among Drosophilids and were found to be dispensable for centromere localization (Fig. 3A; data not shown).

While the regions NLS, AT1, AT2, and the N-terminal domain with the regions R and DH are dispensable for centromere localization, all except AT1 appear to provide other essential functions. Cenp-C versions lacking these regions were unable to prevent phenotypic abnormalities in *Cenp-C* mutant embryos when expressed from appropriate transgenes (data not shown). In contrast, analogous expression of wild-type Cenp-C or Cenp-C lacking AT1 was sufficient to prevent phenotypic abnormalities in *Cenp-C* mutant embryos (Figs. 3A, 6A [below]).

We also analyzed the consequences of overexpression of wild-type and mutant Cenp-C versions during eye and wing development. Overexpression of the minimally

conserved middle region had no effect (Fig. 5, E-M). Overexpression of full-length Cenp-C resulted in an aberrant phenotype but only in wings and not in eyes (Fig. 5, FL and E-FL). Stronger defects were observed after expression of the N-terminal region containing the maximally conserved R and DH blocks (Fig. 5, E-N). The strongest defects were caused by expression of C-terminal regions containing the centromere localization domain (Fig. 5, E-C and E-CN). Therefore, we assume that the overexpressed fragments capable of centromere binding displace wild-type Cenp-C. Similarly, we propose that overexpression of the region with the maximally conserved N-terminal R and DH blocks, as well as an excess of wild-type and thus noncentromeric Cenp-C, might titrate away other components, perhaps kinetochore proteins normally recruited by centromeric wild-type Cenp-C during mitosis.

#### *Is Cenp-C involved in sister-chromatid separation?*

To define the Cenp-C function in further detail, we analyzed the consequences of loss-of-function mutations. In particular, since our identification of *Cenp-C* by genetic interactions argued for a functional cooperation between separase regulatory subunits and this centromere protein, we were interested in whether the *Cenp-C* mutant phenotype provides evidence for a direct interaction.

The two available *Cenp-C* alleles (*prl41* and *IR35*) both behaved as recessive lethal mutations. Homozygous and trans-heterozygous embryos, as well as embryos carrying either of the two alleles over a deficiency (*Df(3R)p25*) did not hatch. Immunolabeling with antibodies against Cyclin B and a DNA stain indicated striking abnormalities within the central nervous system (CNS) during the second half of embryogenesis (Fig. 6A, *Cenp-C*<sup>-</sup>). The CNS of *Cenp-C* mutant embryos included many oversized cells with abnormally high levels of Cyclin B. In addition, pycnotic nuclei characteristic of apoptotic cells were more frequent within the *Cenp-C* mutant CNS, which overall contained far fewer cells than the CNS of wild-type embryos. In contrast, other tissues of *Cenp-C* mutant embryos appeared to be relatively normal. These findings indicated that initial development of *Cenp-C* mutant embryos is normal, presumably reflecting the presence of the maternal *Cenp-C*<sup>+</sup> contribution, which can be demonstrated by immunofluorescence (Fig. 2C), RT-PCR, and immunoblotting experiments (data not shown). However, this maternal *Cenp-C*<sup>+</sup> contribution evidently is no longer sufficient to support the extended cell proliferation known to occur during CNS development, where continued cell cycle progression despite chromosome segregation defects might result in oversized cells and apoptosis in the *Cenp-C* mutants. Accordingly, the observation that the CNS is most severely affected in the *Cenp-C* mutants suggests that Cenp-C is only required in dividing cells. This notion is also supported by the observed correlation between Cenp-C expression and mitotic proliferation (Fig. 2B,C).

To characterize the *Cenp-C* mutant phenotype in fur-

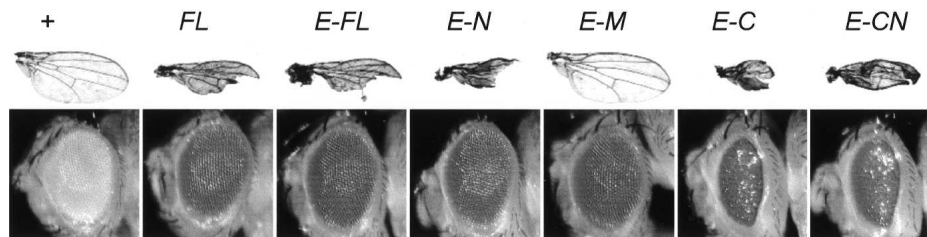


**Figure 5.** Distinct Cenp-C regions cause defects after overexpression. *MS1096* and *GMR-GAL4* were used to drive overexpression of various *UAS-Cenp-C* transgene variants during wing (*top row*) and eye (*bottom row*) development, respectively. Wild-type wings and eyes are present in control flies (+) with a *GAL4* transgene but without an *UAS* transgene. Aberrant wing and eye phenotypes were observed to variable degrees in flies with either *UAS-Cenp-C* II.2 (*FL*), *UAS-EGFP-Cenp-C* II.2 (*E-FL*), *UAS-EGFP-Cenp-C-N* II.1 (*E-N*), *UAS-EGFP-Cenp-C-M* III.2 (*E-M*), *UAS-EGFP-Cenp-C-C* II.1 (*E-C*), or *UAS-EGFP-Cenp-CN* II.2 (*E-CN*) in combination with a *GAL4* transgene. The strongest defects were observed after overexpression of N-terminally truncated Cenp-C fragments containing the centromere localization domain (*E-C* and *E-CN*). However, aberrant wings and eyes were also caused by the N-terminal region, which does not localize to the centromere (*E-N*), while the middle region did not have an effect (*E-M*). Several independent insertions of each transgene variant were analyzed and found to behave similarly to those shown.

ther detail at a cellular level, we focused on the onset of phenotypic abnormalities. Analyses with the two alleles in homo-, hemi-, or trans-heterozygous embryos gave similar results. Starting during embryonic cycle 15, immunolabeling revealed declining Cenp-C levels in *Cenp-C*-deficient embryos compared with sibling controls (data not shown). Based on double-labeling with a DNA stain and scoring of mitotic figures, the division completing cycle 15 appeared still largely normal in the mutants. At the stage of mitosis 16, residual maternally derived Cenp-C levels were further reduced, but still above background at least in some of the mutant embryos (Fig. 2C). However, mitosis 16 was severely affected. Metaphase figures appeared relatively normal,

but anaphase and telophase figures frequently displayed abnormal chromatin bridges (Fig. 6B). Labeling with antibodies against Cid/Cenp-A revealed centromere signals of normal intensity in the *Cenp-C* mutants. Interestingly, in 70% of the chromatin bridges, Cid/Cenp-A signals were observed in the middle (Fig. 6C, *Cenp-C*<sup>-</sup>). Chromatin bridges appearing during mitosis 15 in *Cap-G* mutant embryos almost never displayed comparable central centromere signals (Fig. 6C, *Cap-G*<sup>-</sup>). Cap-G is a subunit of the condensin complex and provides a major function required for sister-chromatid resolution during mitosis. Interestingly, Cap-G has recently been shown to interact genetically and physically with the centromere component Cid/Cenp-A (Jäger et al. 2005). However, the

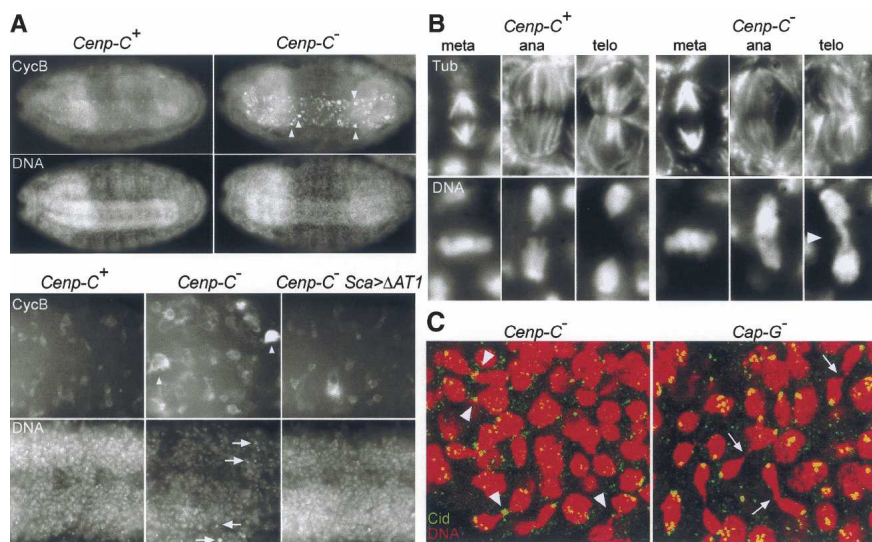


**Figure 6.** *Cenp-C* mutant phenotype. (A) Embryos after germ-band retraction, when mitotic cell proliferation is restricted to the nervous system, were labeled with antibodies against Cyclin B (CycB) and a DNA stain (DNA). While the entire embryos are shown in the two *top rows*, high-magnification views of CNS regions are shown in the two *bottom rows*. In comparison to sibling control embryos (*Cenp-C*<sup>+</sup>), *Cenp-C*<sup>pr141</sup>/*Df(3R)p25* embryos (*Cenp-C*<sup>-</sup>) contain fewer but often much larger cells expressing Cyclin B at very high levels in the central nervous system (arrowheads). In addition, considerably higher numbers of apoptotic cells with pycnotic nuclei are present in these embryos (arrows). *Sca-GAL4*-mediated expression of *UAS-EGFP-Cenp-C* (data not shown) or *UAS-EGFP-Cenp-C-ΔAT1* in the *Cenp-C* mutant embryos (*Cenp-C*<sup>-</sup> *Sca* > *ΔAT1*)

prevents these abnormalities almost completely. (B) Epidermal cells during mitosis 16 from either sibling control embryos (*Cenp-C*<sup>+</sup>) or *Cenp-C*<sup>pr141</sup> mutant embryos (*Cenp-C*<sup>-</sup>) are presented after labeling with antibodies against tubulin (Tub) and a DNA stain (DNA). While metaphase cells (meta) appear to be indistinguishable, anaphase (ana) and telophase (telo) cells frequently displayed chromatin bridges (arrowhead). (C) Epidermal regions after labeling with antibodies against Cid/Cenp-A (Cid, green) and a DNA stain (DNA, red) contain late mitotic cells with chromatin bridges in both *Cenp-C*<sup>pr141</sup>/*Cenp-C*<sup>LR35</sup> (*Cenp-C*<sup>-</sup>) and *Cap-G*<sup>6</sup>/*Df(2R)vg56* (*Cap-G*<sup>-</sup>) mutant embryos. However, while the majority of the chromatin bridges in *Cenp-C*<sup>-</sup> embryos display anti-Cid/Cenp-A signals at the midpoint (arrowheads), bridges in *Cap-G*<sup>-</sup> embryos are devoid of such signals (arrows).

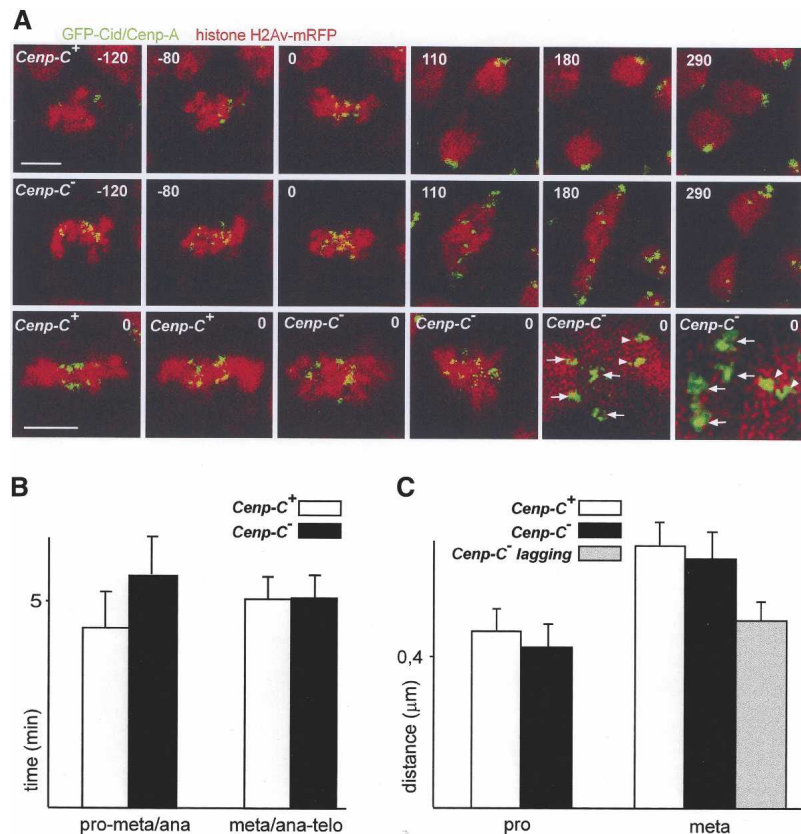
early phenotypic consequences of mutations in *Cenp-C* and *Cap-G* are evidently distinct.

Our observations in fixed mutant embryos indicated that *Cenp-C* is particularly important for separation of sister centromeres during mitosis and/or for segregation of sister chromatids to the poles. A distinct increase in the number of phospho-histone H3-positive cells was observed after incubation in colchicine, demonstrating that the mitotic spindle checkpoint is still functional in *Cenp-C* mutants, at least in most cells at the stage of mitosis 16. Nevertheless, immunolabeling with an antibody against the checkpoint component BubR1 already revealed less intense signals at the kinetochores during prometaphase 16 in *Cenp-C* mutants compared with sibling controls (data not shown). Moreover, the relatively normal appearance and number of metaphase plates during mitosis 16 in the *Cenp-C* mutants also argued that most kinetochores are still quite functional, allowing for chromosome attachment to the mitotic spindle, chromosome congression into the metaphase plate, and spindle checkpoint silencing.

Since kinetochore functionality in *Cenp-C* mutants

would be surprising and a strong argument for a sister separation defect as an underlying cause of the observed anaphase defects, we applied *in vivo* imaging for a more careful analysis of kinetochore functionality, in particular in sister-chromatid pairs that fail to become segregated during mitosis 16 in *Cenp-C* mutants. Therefore, we crossed transgenes driving expression of mRFP fused to histone H2Av and EGFP fused to Cid/Cenp-A into the *Cenp-C* mutant background. Time-lapse analysis of progression through mitosis 16 (Fig. 7) clearly revealed that chromosome congression into a metaphase plate is slightly delayed in the mutants. The period from the onset of chromosome condensation until the metaphase-to-anaphase transition lasted for ~5.6 min in the *Cenp-C* mutants, compared with 4.4 min in sibling controls (Fig. 7B). This delay occurred during prometaphase. Moreover, the metaphase frame acquired just before the onset of anaphase usually revealed a more irregular centromere positioning than in the straight metaphase plates characteristically observed in sibling control embryos (Fig. 7A). After the metaphase-to-anaphase transition, some mutant cells failed to achieve timely separation and/or

**Figure 7.** Mitotic chromosome segregation in *Cenp-C* mutant embryos. (A) Mitotic divisions in *Cenp-C*<sup>+</sup> (*Cenp-C*<sup>+</sup>) or *Cenp-C*<sup>-</sup> (*Cenp-C*<sup>-</sup>) embryos expressing *gcid-EGFP-cid* (GFP-Cid/Cenp-A) and *His2Av-mRFP1* (histone H2Av-mRFP) were analyzed by time-lapse *in vivo* imaging. The time (in seconds) relative to the last frame before the onset of anaphase, which was set to 0, is indicated in each frame. All frames in the *top* row are from a cell progressing through mitosis 16 in a *Cenp-C*<sup>+</sup> sibling control embryo and all frames in the *middle* row from a *Cenp-C*<sup>-</sup> embryo at the same stage. Magnification in the *top* two rows is indicated by the white bar in the *upper left* panel, which corresponds to 3  $\mu$ m. Various metaphase plates are shown in the *bottom* row always in the same orientation with the bar corresponding to 3  $\mu$ m illustrating the magnification shown in the first four panels. Even higher magnifications are shown in the two *right-most* panels in which sister centromeres of lagging chromosomes in *Cenp-C*<sup>-</sup> embryos are indicated by white arrowheads and those of nonlagging chromosomes by white arrows. Chromosomes that were subsequently lagging behind during anaphase in *Cenp-C*<sup>-</sup> embryos did not only have more closely spaced sister centromeres than nonlagging chromosomes (see also C) but were also often not oriented in the axis of the spindle, as evident in the *right-most* panel in the *bottom* row. (B) The average time (in minutes) from the onset of mitosis 16 until the last frame before the onset of anaphase (pro-meta/ana), as well as from the onset of anaphase until telophase (meta/ana-telo), was determined after time-lapse analysis of embryos that were either *Cenp-C*<sup>+</sup> (*Cenp-C*<sup>+</sup>, white bars) or *Cenp-C*<sup>-</sup> (*Cenp-C*<sup>-</sup>, black bars). At least 20 mitoses from more than four embryos were analyzed. (C) The distance between sister centromeres (in micrometers) was determined during prophase (pro) and immediately before the onset of anaphase (meta) after time-lapse analysis of embryos at the stage of mitosis 16. Average values obtained with *Cenp-C*<sup>+</sup> embryos are represented by white bars. Values obtained for chromosomes that were subsequently lagging behind during anaphase in *Cenp-C*<sup>-</sup> embryos are indicated by the gray bar, while the values observed in *Cenp-C*<sup>-</sup> embryos during prophase and before the metaphase-to-anaphase transition in case of nonlagging chromosomes are given by black bars. At least 11 chromosomes from more than four embryos were analyzed.



segregation of one or two chromosomes (Fig. 7A). Measuring the distance between the sister kinetochores just before the metaphase-to-anaphase transition indicated that these late or nonsegregating chromosomes were not attached to the spindle in a normal bipolar fashion. Bipolar attachment results in a significant increase in the intersister kinetochore distance, as confirmed by comparing the values in sibling control embryos during prophase and metaphase (Fig. 7C). This increase was also observed in the *Cenp-C* mutants but only in the normally segregating chromosomes. In contrast, in the non-segregating chromosomes, the intersister kinetochore distance at the metaphase-to-anaphase transition was not greater than the average distance observed during prophase (Fig. 7C). These findings indicate that Cenp-C is required for normal bipolar kinetochore attachment.

## Discussion

Our identification of *Drosophila* Cenp-C closes a prominent gap in the arguments for homologous centromere organization. Centromeric DNA sequences have evolved extremely rapidly and appear to have driven the coevolution of centromeric proteins during eukaryote evolution (Henikoff et al. 2001; Talbert et al. 2004). The resulting low sequence similarity between centromeric proteins has effectively concealed the existence of a common set of constitutive eukaryotic centromere proteins until very recently. The first features demonstrated to be shared among fungal, plant, and animal centromeres were centromere-specific histone H3 variants (Sullivan et al. 1994; Stoler et al. 1995; Buchwitz et al. 1999; Henikoff et al. 2000; Takahashi et al. 2000; Talbert et al. 2002). In addition to these Cenp-A homologs, only one further constitutive centromere component, Cenp-C, has so far been shown to be present in each of the three main eukaryotic branches (Saitoh et al. 1992; Brown 1995; Meluh and Koshland 1995; Dawe et al. 1999; Moore and Roth 2001; Talbert et al. 2004). Our findings now also establish the existence of *Drosophila* Cenp-C, which had previously escaped detection by careful bioinformatics genome analyses (Talbert et al. 2004) because of its very limited sequence similarity. In combination with the recent identification of related Cenp-H-, Cenp-I-, and Mis12-like proteins in both vertebrates and yeast (Nishihashi et al. 2002; Goshima et al. 2003; Westermann et al. 2003; Cheeseman et al. 2004; Obuse et al. 2004), our results provide strong support for the notion of a common set of constitutive centromere proteins. These proteins, which are centromeric throughout the cell cycle, appear to provide a foundation for kinetochore assembly and spindle attachment during mitosis by recruiting several distinct multisubunit complexes that also contain highly diverged proteins (Wigge and Kilmartin 2001; De Wulf et al. 2003; Westermann et al. 2003; Cheeseman et al. 2004).

The extensive sequence divergence characteristically observed among homologous eukaryotic centromere and kinetochore proteins is striking, especially in the light of their common fundamental cellular function. The aver-

age amino acid identity observed in a genome-wide comparison of *D. melanogaster* and *D. pseudoobscura* ortholog pairs is 77% (Richards et al. 2005) and only 38% in case of the *Cenp-C* pair. Moreover, based on the ratio between radical charge mutations and conservative substitutions in *D. melanogaster* and *D. pseudoobscura* ortholog pairs, *Cenp-C* is one of 44 genes likely to have evolved under positive selection (Richards et al. 2005). Except for a few very restricted regions (data not shown), our comparison of *D. melanogaster* *Cenp-C* with the orthologs from *D. erecta* and *D. yakuba*, which are closer relatives than *D. pseudoobscura* and thus amenable to  $d_N/d_S$  analyses (Comeron 1999), did not reveal strong evidence for positive selection, in contrast to the recent findings in plant and mammalian lineages (Talbert et al. 2004). However, we point out that these  $d_N/d_S$  analyses ignore insertions and deletions (indels), which have occurred considerably more often during *Cenp-C* evolution in Drosophilids than in the mammalian lineage. Most of the indels are observed within the minimally conserved central regions of Drosophilid Cenp-C. Similar variabilities resulting from recurrent exon duplications have been observed in the central region of the plant Cenp-C genes (Talbert et al. 2004).

The adaptively evolving regions of mammalian Cenp-C have been shown to bind to DNA in vitro, consistent with the proposed coevolution of centromeric DNA and protein sequences (Talbert et al. 2004). However, this DNA binding in vitro is not sequence-specific (Sugimoto et al. 1994), suggesting that interactions with centromere-specific proteins contribute to centromere localization of Cenp-C. As in other organisms (Howman et al. 2000; Moore and Roth 2001; Oegema et al. 2001; Van Hooser et al. 2001; Westermann et al. 2003), Cid/Cenp-A is also required for centromere localization of Cenp-C in *Drosophila*. High-resolution light microscopy of mitotic chromosomes has indicated that human Cenp-C covers the poleward-oriented peripheral region of the Cenp-A-containing centromeric chromatin (Blower et al. 2002). Direct interactions between Cenp-A and Cenp-C have not yet been demonstrated in any organism. Our attempts with yeast two-hybrid experiments were also unsuccessful (R. Schittenhelm, S. Heeger, and C.F. Lehner, unpubl.).

The CENPC motif has recently been identified as the only region conserved among the Cenp-C orthologs from fungi, plant, and animals (Talbert et al. 2004). In Drosophilids, even this short motif of ~24 amino acids is not fully conserved in its C-terminal part. Our results suggest that this CENPC motif is crucial for centromere localization. We demonstrate that a single-point mutation affecting one of the invariant positions in the CENPC motif interferes with centromere localization of the C-terminal domain of Cenp-C in our transfection assay. This mutation was identified as the only missense mutation interfering with centromere localization after extensive random mutagenesis. Further experiments will reveal whether and how the CENPC motif contacts Cid/Cenp-A nucleosomes. We would like to emphasize, however, that also in *Drosophila* Cenp-C, other regions

than the CENPC motif clearly contribute to efficient centromere localization. Centromere localization of the CN subregion (1009–1205), for instance, is only detected in our transfection assay in live but not in fixed cells, while centromere localization of the larger C region (1009–1411) is resistant to fixation.

The highest conservation among Drosophilid Cenp-C proteins is observed within the N-terminal third, which is neither required nor sufficient for normal centromere localization. Nevertheless, prolonged overexpression of this domain in proliferating eye and wing imaginal disc cells results in severe defects. The conserved N-terminal Cenp-C domains (R and DH) might bind to kinetochore proteins and titrate these away from the centromere when overexpressed. Biochemical and genetic characterizations in *Saccharomyces cerevisiae* and *Caenorhabditis elegans* have suggested that Cenp-C is not only associated with Cenp-A, but that it also recruits the next layer of kinetochore proteins, in particular the Mis12/Mtw1 and Ndc80 complexes, which remain to be identified in *Drosophila* (De Wulf et al. 2003; Pinsky et al. 2003; Westermann et al. 2003; Cheeseman et al. 2004).

As in yeast (Meluh and Koshland 1995), chicken (Fukagawa and Brown 1997; Fukagawa et al. 1999), and mice (Kalitsis et al. 1998), *Cenp-C* is also an essential gene in *Drosophila*. Antibody microinjection experiments in mammalian cells (Tomkiel et al. 1994); RNA interference in *C. elegans* (Moore and Roth 2001; Oegema et al. 2001); and phenotypic analysis in yeast (Brown et al. 1993), chicken cells (Fukagawa et al. 2001), and mutant *Drosophila* embryos demonstrate that Cenp-C is required for normal chromosome segregation during mitosis. Our *in vivo* imaging in *Cenp-C* mutant embryos discloses these defects in detail. Previously, *in vivo* imaging has also been applied in *C. elegans* *CENP-C(RNAi)* embryos (Moore and Roth 2001; Oegema et al. 2001). The formation of holocentric chromosomes and transient Cenp-C recruitment only during mitosis differentiates *C. elegans* from other metazoans like *Drosophila* and mammalian cells. Moreover, in contrast to the findings in *C. elegans*, chromosome congression into a central plane is still observed in the *Drosophila* *Cenp-C* mutants. Presumably, this chromosome congression reflects the function of residual maternally provided Cenp-C, which is still detectable at the stage of our analyses. Moreover, our time-lapse analyses demonstrate that chromosome congression is not entirely normal in the *Cenp-C* mutant embryos. Metaphase plate formation is delayed and often does not lead to the highly ordered arrangement of all chromosomes characteristically observed before anaphase onset in wild type. Occasional chromosomes fail to achieve bipolar attachment in the *Cenp-C* mutants. These chromosomes do not segregate normally during anaphase. Cenp-C is, therefore, clearly required for normal attachment of kinetochores to the mitotic spindle.

Evidently, the insufficiently attached chromosomes in *Cenp-C* mutant embryos are unable to inhibit the onset of anaphase, even though the mitotic spindle checkpoint appears to be at least partially functional in *Cenp-C* mu-

tants at the analyzed stage. However, assembly of mitotic spindle checkpoint proteins might fail, particularly on the kinetochores of those chromosomes that do not attach correctly to the mitotic spindle.

In principle, the chromosome segregation defects observed in the *Cenp-C* mutants might not only reflect impaired interactions between kinetochores and spindle. Segregation of sister chromatids to the spindle poles also depends on complete resolution of sister-chromatid cohesion at the metaphase-to-anaphase transition. This final separation of sister chromatids is thought to be achieved by separase-mediated cleavage of the Scc1/Rad21 subunit of those cohesin complexes that perdure in the pericentromeric region until the metaphase-to-anaphase transition. Several observations are consistent with the idea that a localized full activation of separase might be assisted by centromeric proteins (see above). Accordingly, mutations in *Cenp-C* might reduce separase activity and thereby explain the genetic interactions with the regulatory separase subunits Pim/securin and Thr that led to our identification of *Drosophila* Cenp-C. We have failed to observe coimmunoprecipitation of Cenp-C with separase complex proteins and have been unable to detect effects of *Cenp-C* mutations on Pim and Thr levels (O. Leismann and C.F. Lehner, unpubl.). Our analysis has, therefore, not exposed clear evidence for separase activation at centromeres. On the other hand, Cenp-C is clearly required for normal chromosome attachment to the mitotic spindle, and thus the observed genetic interactions most likely reflect a summation of negative effects on the efficiency of sister-chromatid separation (by separase) and segregation (by the spindle). However, we would like to emphasize that our results certainly do not rule out a local activation of separase within the centromeric region.

## Materials and methods

### Fly stocks

We used the *GAL4* driver lines *GMR-GAL4*, *MS1096*, *Sc-GAL4*, *2xsev-Hs-GAL4* 332.5. *UAS-pim-myc* (Leismann et al. 2000), and *UAS-cid* (Jäger et al. 2005) have been described previously. For the generation of *GMR-thrΔC* lines, we used a pGMR construct (Hay et al. 1994) containing the same insert fragment including the myc-epitope region as present in *UAS-thr1-930-myc* (Jäger et al. 2001). The deficiency kit, as well as *Df(3R)Exel6149*, was obtained from the Bloomington *Drosophila* Stock Center. Its composition at the time of our screen, as well as a list of the deficiencies that were identified as dominant modifiers of the adult rough eye phenotype resulting from *GMR-thrΔC* or *GMR-GAL4 UAS-pim-myc* expression is given in the Supplemental Material. *l(3)85Aa<sup>pp141</sup>* (Jones and Rawls 1988) was also obtained from the Bloomington *Drosophila* Stock Center. *l(3)85Aa<sup>IR35</sup>* was kindly provided by K. Dej and T. Orr-Weaver (The Whitehead Institute, Cambridge, MA). *cid<sup>12-1</sup>* and *cid<sup>12-4</sup>* were generously provided by Thom Kaufman (Indiana University, Bloomington) and used for the analysis of Cenp-C localization in trans-heterozygous embryos. *Cap-G<sup>6</sup>* (Jäger et al. 2005) was crossed over *Df(2R)vg56* for the phenotypic comparison with *Cenp-C* mutants. The *His2Av-mRFP1*

and the *gcid-EGFP-cid* transgenic lines, which express functional fusion proteins as assessed by mutant rescue experiments, will be described in detail elsewhere.

Lines carrying genomic fragments from the 85A region were constructed for the identification of the locus interacting with eye-specific *pim* and *thrΔC* overexpression, using insert DNA derived from the BAC clone R48A14 (Hoskins et al. 2000) and pCaSpeR4 followed by standard P element germline transformation. Three olfactory receptor genes (*Or85b*, *Or85c*, *Or85d*) within the region delimited by deficiency breakpoints were excluded from further analysis. A transgene containing a 15-kb fragment with the predicted genes *CG11737*, *CG31454*, and *CG31259* did not prevent the lethality of the *l(3)85A<sup>pr141</sup>* mutants. The *abcd* transgene contained a 14.6-kb NdeI-XbaI fragment including *CG31453*, *mRpS18C*, *CG31460*, and *Cenp-C*. The same fragment after filling and religation of a SalI site within exon 5 of *Cenp-C* was used in the *abcd<sup>m</sup>* transgene. The proximal 6.4-kb NdeI-EcoRI subfragment lacking *Cenp-C* was used in the *abc* transgene, and the *d* transgene contained the distal 8.7-kb PmlI-XbaI subfragment including only *Cenp-C*.

For the expression of *Cenp-C* fused to EYFP or 10 copies of the myc epitope under control of the *Cenp-C* regulatory region, we modified the *d* transgene construct for the generation of the *gEYFP-Cenp-C* and *gmyc-Cenp-C* lines. A slightly larger subfragment (10.3-kb StuI-XbaI fragment) was used for the *gCenp-C-EGFP* and *gCenp-C-myc* lines. While *gCenp-C-EGFP*, *gmyc-Cenp-C*, and *gCenp-C-myc* insertions were unable to confer full rescue when crossed into *Cenp-C* mutant backgrounds, *gEYFP-Cenp-C* allowed *Cenp-C* mutant development to the adult stage.

The vector pUAST (Brand and Perrimon 1993) and the EST clone RE27988 (Berkeley *Drosophila* Genome Project), which contains a full-length *Cenp-C* cDNA insert according to our sequence analyses, were used for the generation of transgenic lines allowing *GAL4*-dependent expression of wild-type and mutant *Cenp-C* versions (Fig. 3). Moreover, the EGFP coding sequence was introduced into these transgenes immediately after the start codon.

#### Mutagenesis and transfection

The GeneMorph II random mutagenesis kit (Stratagene) was used for the enzymatic amplification of a *Cenp-C* cDNA region under mutagenic conditions using the primers mf (5'-ACGAGCTGTACAAGCTTGCC-3') and mr (5'-GCAACCGAAGATATCATAGGC-3') and the plasmid pRS1 as template. This pBluescript KS+ derivative contained the Gal4-binding sites and the basal *Hsp70Bb* promoter region isolated from pUAST upstream of the *EGFP-Cenp-C-C* (amino acids 1009–1411) fusion gene. The amplification products were digested with HindIII and EcoRV and used to replace the corresponding 668-bp region in pRS1, resulting in a mutant clone library after electroporation of *Escherichia coli* DH10B cells. The QIAprep 96 Turbo Miniprep kit (QIAGEN) was used for the preparation of plasmid DNA from 394 random clones.

Expression of the mutant library was achieved by transfection of *Drosophila* SR+ cells (Yanagawa et al. 1998). These cells were cultured at 26°C in Schneider's *Drosophila* Medium (GIBCO) containing 10% fetal bovine serum, 1% penicillin, and 1% streptomycin. Before transfection, we plated 10<sup>5</sup> cells/well of a μClear 96 well plate (GIBCO) in 0.2 mL of medium. After 24 h, medium was exchanged with 0.16 mL of fresh medium and 0.04 mL of transfection mix containing 0.25 μg of a given mutant library plasmid, 0.75 μg of pBluescript KS+ as carrier DNA, and 3 μL of FuGene6 (Roche) in Dulbecco's Modified Eagle's Medium (GIBCO). EGFP signals were analyzed 24 h after transfection

in live cells using an inverted confocal laser scanning microscope (Leica DM IRBE TCS SP1) with a 40× oil immersion objective. Initial experiments involving transfection of the same pUAST-EGFP-Cenp-C constructs that had previously been analyzed after *Drosophila* germline transformation indicated that the subcellular localization of these mutant Cenp-C versions (FL, N, M, C, CN, CM, CC, ΔN, ΔAT1, ΔNLS, ΔAT2) (see Fig. 3) in SR+ cells was identical as in transgenic embryos. In initial experiments, cotransfection of pUAST-EGFP-Cenp-C constructs with an Act5c-GAL4 plasmid resulted in very high levels of expression, which obscured centromere localization in many cases. The Act5c-GAL4 plasmid was therefore omitted in subsequent experiments, and basal expression of the pUAST derivatives proved to be sufficient for detection of centromere localization.

#### In vivo imaging and immunofluorescence

Syncytial blastoderm-stage embryos of a *gEYFP-Cenp-C* II.1; *His2Av-mRFP1* III.1 line were analyzed by in vivo imaging essentially as described previously (Pandey et al. 2005). Moreover, embryos obtained from a cross of *His2Av-mRFP1* II.2, *gcid-EGFP-cid* II.1; *Cenp-C<sup>pr141</sup>/TM3*, *Sb*, *Kr-GAL4*, *UAS-GFP* females with *Cenp-C<sup>IR35</sup>/TM3*, *Sb*, *Kr-GAL4*, *UAS-GFP* males were analyzed analogously at the stage when the epidermal cells progress through mitosis 16.

Immunofluorescence and DNA labeling of fixed embryos was performed essentially as described previously (Leismann et al. 2000). Affinity-purified rabbit antibodies against Cid/Cenp-A (Jäger et al. 2005), Cyclin B (Jacobs et al. 1998), and GFP (Molecular Probes Inc.), and mouse monoclonal antibodies against α-tubulin DM1A (Sigma) were used at a dilution of 1:500, 1:500, 1:5000, and 1:8000, respectively. An affinity-purified rabbit antibody against *Drosophila* Cenp-C was generated with a bacterially expressed protein fragment (amino acids 502–939) with a His-tag and used at a dilution of 1:5000. For the analysis of the CNS phenotype, 12–14-h embryos were collected from a cross of *Sca-GAL4*; *Df(3R)p25/TM3*, *Sb*, *P{35Ubx-lacZ}/2* males and *Cenp-C<sup>pr141</sup>/TM3*, *Sb*, *P{35Ubx-lacZ}/2* females with or without a *UAS-EGFP-Cenp-C* transgene. *Cenp-C<sup>pr141</sup>/Df(3R)p25* embryos were identified after double-labeling with antibodies against β-galactosidase.

#### Sequence comparisons

The VISTA Browser (Couronne et al. 2003) and the *Drosophila* Species Genome Web pages (<http://bugbane.bio.indiana.edu:7151>) were used for the identification of *Cenp-C* genes in genome sequences of *D. ananassae*, *D. erecta*, *D. pseudoobscura*, *D. simulans*, *D. virilis*, and *D. yakuba* (prepublication data from Agencourt Bioscience Corporation and Genome Sequencing Center at Washington University; Richards et al. 2005). Alignments of coding and amino acid sequences were performed using the European Bioinformatics Institute CLUSTAL W Server (Thompson et al. 1994). Cenp-C-box consensus motifs were displayed using the Logos program on the Blocks WWW Server (<http://blocks.fhcr.org>). K-estimator (Comeron 1999) was used for *d<sub>N</sub>/d<sub>S</sub>* analyses that estimate and compare the rate of non-synonymous and synonymous exchanges in *Cenp-C* gene pairs from closely related species. Prior to analysis, insertions were removed from the coding sequences.

#### Acknowledgments

We are most grateful to Kim Dej and Terry Orr-Weaver for communicating unpublished information and generously providing

the IR35 allele. We are also indebted to Thom Kaufman for unpublished information and the *cid* mutant strains. We thank Buzz Baum for providing the SR+ cells, as well as Matthias Fischer and Rahul Pandey for their contributions during preparation of anti-Cenp-C antibodies and immunoblotting, and many other lab members for additional help. This work was supported by a grant from the Deutsche Forschungsgemeinschaft (DFG Le 987/3-3) and by the Fonds der Deutschen Chemie.

## References

- Blower, M.D., Sullivan, B.A., and Karpen, G.H. 2002. Conserved organization of centromeric chromatin in flies and humans. *Dev. Cell* **2**: 319–330.
- Brand, A.H. and Perrimon, N. 1993. Targeted gene expression as a means of altering cell fates and generating dominant phenotypes. *Development* **118**: 401–415.
- Brown, M.T. 1995. Sequence similarities between the yeast chromosome segregation protein Mif2 and the mammalian centromere protein CENP-C. *Gene* **160**: 111–116.
- Brown, M.T., Goetsch, L., and Hartwell, L.H. 1993. MIF2 is required for mitotic spindle integrity during anaphase spindle elongation in *Saccharomyces cerevisiae*. *J. Cell Biol.* **123**: 387–403.
- Buchwitz, B.J., Ahmad, K., Moore, L.L., Roth, M.B., and Henikoff, S. 1999. A histone-H3-like protein in *C. elegans*. *Nature* **401**: 547–548.
- Cheeseman, I.M., Niessen, S., Anderson, S., Hyndman, F., Yates III, J.R., Oegema, K., and Desai, A. 2004. A conserved protein network controls assembly of the outer kinetochore and its ability to sustain tension. *Genes & Dev.* **18**: 2255–2268.
- Chestukhin, A., Pfeffer, C., Milligan, S., DeCaprio, J.A., and Pellman, D. 2003. Processing, localization, and requirement of human separase for normal anaphase progression. *Proc. Natl. Acad. Sci.* **100**: 4574–4579.
- Ciosk, R., Zachariae, W., Michaelis, C., Shevchenko, A., Mann, M., and Nasmyth, K. 1998. An ESP1/PDS1 complex regulates loss of sister chromatid cohesion at the metaphase to anaphase transition in yeast. *Cell* **93**: 1067–1076.
- Comeron, J.M. 1999. K-Estimator: Calculation of the number of nucleotide substitutions per site and the confidence intervals. *Bioinformatics* **15**: 763–764.
- Couronne, O., Poliakov, A., Bray, N., Ishkhanov, T., Ryaboy, D., Rubin, E., Pachter, L., and Dubchak, I. 2003. Strategies and tools for whole-genome alignments. *Genome Res.* **13**: 73–80.
- Dawe, R.K., Reed, L.M., Yu, H.G., Muszynski, M.G., and Hiatt, E.N. 1999. A maize homolog of mammalian CENPC is a constitutive component of the inner kinetochore. *Plant Cell* **11**: 1227–1238.
- De Wulf, P., McAinsh, A.D., and Sorger, P.K. 2003. Hierarchical assembly of the budding yeast kinetochore from multiple subcomplexes. *Genes & Dev.* **17**: 2902–2921.
- Earnshaw, W.C. and Rothfield, N. 1985. Identification of a family of human centromere proteins using autoimmune sera from patients with scleroderma. *Chromosoma* **91**: 313–321.
- Fukagawa, T. and Brown, W.R. 1997. Efficient conditional mutation of the vertebrate CENP-C gene. *Hum. Mol. Genet.* **6**: 2301–2308.
- Fukagawa, T., Pendon, C., Morris, J., and Brown, W. 1999. CENP-C is necessary but not sufficient to induce formation of a functional centromere. *EMBO J.* **18**: 4196–4209.
- Fukagawa, T., Regnier, V., and Ikemura, T. 2001. Creation and characterization of temperature-sensitive CENP-C mutants in vertebrate cells. *Nucleic Acids Res.* **29**: 3796–3803.
- Funabiki, H., Kumada, K., and Yanagida, M. 1996. Fission yeast Cut1 and Cut2 are essential for sister separation, concentrate along the metaphase spindle and form large complexes. *EMBO J.* **15**: 6617–6628.
- Goshima, G., Kiyomitsu, T., Yoda, K., and Yanagida, M. 2003. Human centromere chromatin protein hMis12, essential for equal segregation, is independent of CENP-A loading pathway. *J. Cell Biol.* **160**: 25–39.
- Hay, B.A., Wolff, T., and Rubin, G.M. 1994. Expression of baculovirus p35 prevents cell-death in *Drosophila*. *Development* **120**: 2121–2129.
- Henikoff, S., Ahmad, K., Platero, J.S., and van Steensel, B. 2000. Heterochromatic deposition of centromeric histone H3-like proteins. *Proc. Natl. Acad. Sci.* **97**: 716–721.
- Henikoff, S., Ahmad, K., and Malik, H.S. 2001. The centromere paradox: Stable inheritance with rapidly evolving DNA. *Science* **293**: 1098–1102.
- Herzig, A., Lehner, C.F., and Heidmann, S. 2002. Proteolytic cleavage of the THR subunit during anaphase limits *Drosophila* separase function. *Genes & Dev.* **16**: 2443–2454.
- Hoskins, R.A., Nelson, C.R., Berman, B.P., Laverty, T.R., George, R.A., Ciesiolka, L., Naemuddin, M., Arenson, A.D., Durbin, J., David, R.G., et al. 2000. A BAC-based physical map of the major autosomes of *Drosophila melanogaster*. *Science* **287**: 2271–2274.
- Howman, E.V., Fowler, K.J., Newson, A.J., Redward, S., MacDonald, A.C., Kalitsis, P., and Choo, K.H. 2000. Early disruption of centromeric chromatin organization in centromere protein A (Cenpa) null mice. *Proc. Natl. Acad. Sci.* **97**: 1148–1153.
- Jacobs, H.W., Knoblich, J.A., and Lehner, C.F. 1998. *Drosophila* Cyclin B3 is required for female fertility and is dispensable for mitosis like Cyclin B. *Genes & Dev.* **12**: 3741–3751.
- Jäger, H., Herzig, A., Lehner, C.F., and Heidmann, S. 2001. *Drosophila* separase is required for sister chromatid separation and binds to PIM and THR. *Genes & Dev.* **15**: 2572–2584.
- Jäger, H., Herzig, B., Herzig, A., Sticht, H., Lehner, C.F., and Heidmann, S. 2004. Structure predictions and interaction studies indicate homology of separase N-terminal regulatory domains and *Drosophila* THR. *Cell Cycle* **3**: 182–188.
- Jäger, H., Rauch, M., and Heidmann, S. 2005. The *Drosophila melanogaster* condensin subunit Cap-G interacts with the centromere-specific histone H3 variant CID. *Chromosoma* **113**: 350–361.
- Jensen, S., Segal, M., Clarke, D.J., and Reed, S.I. 2001. A novel role of the budding yeast separin Esp1 in anaphase spindle elongation: Evidence that proper spindle association of Esp1 is regulated by Pds1. *J. Cell Biol.* **152**: 27–40.
- Jones, W.K. and Rawls Jr., J.M. 1988. Genetic and molecular mapping of chromosome region 85A in *Drosophila melanogaster*. *Genetics* **120**: 733–742.
- Kalitsis, P., Fowler, K.J., Earle, E., Hill, J., and Choo, K.H. 1998. Targeted disruption of mouse centromere protein C gene leads to mitotic disarray and early embryo death. *Proc. Natl. Acad. Sci.* **95**: 1136–1141.
- Kumada, K., Nakamura, T., Nagao, K., Funabiki, H., Nakagawa, T., and Yanagida, M. 1998. Cut1 is loaded onto the spindle by binding to Cut2 and promotes anaphase spindle movement upon Cut2 proteolysis. *Curr. Biol.* **8**: 633–641.
- Lanini, L. and McKeon, F. 1995. Domains required for CENP-C assembly at the kinetochore. *Mol. Biol. Cell* **6**: 1049–1059.
- Leismann, O., Herzig, A., Heidmann, S., and Lehner, C.F. 2000. Degradation of *Drosophila* PIM regulates sister chromatid separation during mitosis. *Genes & Dev.* **14**: 2192–2205.
- Meeks-Wagner, D., Wood, J.S., Garvik, B., and Hartwell, L.H. 1986. Isolation of two genes that affect mitotic chromosome

- transmission in *S. cerevisiae*. *Cell* **44**: 53–63.
- Meluh, P.B. and Koshland, D. 1995. Evidence that the MIF2 gene of *Saccharomyces cerevisiae* encodes a centromere protein with homology to the mammalian centromere protein CENP-C. *Mol. Biol. Cell* **6**: 793–807.
- Moore, L.L. and Roth, M.B. 2001. HCP-4, a CENP-C-like protein in *Caenorhabditis elegans*, is required for resolution of sister centromeres. *J. Cell Biol.* **153**: 1199–1208.
- Nasmyth, K. 2002. Segregating sister genomes: The molecular biology of chromosome separation. *Science* **297**: 559–565.
- Nishihashi, A., Haraguchi, T., Hiraoka, Y., Ikemura, T., Regnier, V., Dodson, H., Earnshaw, W.C., and Fukagawa, T. 2002. CENP-I is essential for centromere function in vertebrate cells. *Dev. Cell* **2**: 463–476.
- Obuse, C., Iwasaki, O., Kiyomitsu, T., Goshima, G., Toyoda, Y., and Yanagida, M. 2004. A conserved Mis12 centromere complex is linked to heterochromatic HP1 and outer kinetochore protein Zwint-1. *Nat. Cell Biol.* **6**: 1135–1141.
- Oegema, K., Desai, A., Rybina, S., Kirkham, M., and Hyman, A.A. 2001. Functional analysis of kinetochore assembly in *Caenorhabditis elegans*. *J. Cell Biol.* **153**: 1209–1226.
- Pandey, R., Heidmann, S., and Lehner, C.F. 2005. Epithelial reorganization and dynamics of progression through mitosis in *Drosophila* separase complex mutants. *J. Cell Sci.* **118**: 733–742.
- Pinsky, B.A., Tatsutani, S.Y., Collins, K.A., and Biggins, S. 2003. An Mtw1 complex promotes kinetochore biorientation that is monitored by the Ipl1/Aurora protein kinase. *Dev. Cell* **5**: 735–745.
- Richards, S., Liu, Y., Bettencourt, B.R., Hradecky, P., Letovsky, S., Nielsen, R., Thornton, K., Hubisz, M.J., Chen, R., Meisel, R.P., et al. 2005. Comparative genome sequencing of *Drosophila pseudoobscura*: Chromosomal, gene, and cis-element evolution. *Genome Res.* **15**: 1–18.
- Saitoh, H., Tomkiel, J., Cooke, C.A., Ratrie III, H., Maurer, M., Rothfield, N.F., and Earnshaw, W.C. 1992. CENP-C, an autoantigen in scleroderma, is a component of the human inner kinetochore plate. *Cell* **70**: 115–125.
- Shibata, F. and Murata, M. 2004. Differential localization of the centromere-specific proteins in the major centromeric satellite of *Arabidopsis thaliana*. *J. Cell Sci.* **117**: 2963–2970.
- Song, K., Gronemeyer, B., Lu, W., Eugster, E., and Tomkiel, J.E. 2002. Mutational analysis of the central centromere targeting domain of human centromere protein C (CENP-C). *Exp. Cell Res.* **275**: 81–91.
- Stoler, S., Keith, K.C., Curnick, K.E., and Fitzgerald-Hayes, M. 1995. A mutation in *CSE4*, an essential gene encoding a novel chromatin-associated protein in yeast, causes chromosome nondisjunction and cell-cycle arrest at mitosis. *Genes & Dev.* **9**: 573–586.
- Sugimoto, K., Yata, H., Muro, Y., and Himeno, M. 1994. Human centromere protein C (CENP-C) is a DNA-binding protein which possesses a novel DNA-binding motif. *J. Biochem. (Tokyo)* **116**: 877–881.
- Sullivan, K.F., Hechenberger, M., and Masri, K. 1994. Human CENP-A contains a histone H3 related histone fold domain that is required for targeting to the centromere. *J. Cell Biol.* **127**: 581–592.
- Takahashi, K., Chen, E.S., and Yanagida, M. 2000. Requirement of Mis6 centromere connector for localizing a CENP-A-like protein in fission yeast. *Science* **288**: 2215–2219.
- Talbert, P.B., Masuelli, R., Tyagi, A.P., Comai, L., and Henikoff, S. 2002. Centromeric localization and adaptive evolution of an *Arabidopsis* histone H3 variant. *Plant Cell* **14**: 1053–1066.
- Talbert, P.B., Bryson, T.D., and Henikoff, S. 2004. Adaptive evolution of centromere proteins in plants and animals. *J. Biol.* **3**: 18.
- Thompson, J.D., Higgins, D.G., and Gibson, T.J. 1994. CLUSTAL W: Improving the sensitivity of progressive multiple sequence alignment through sequence weighting, position-specific gap penalties and weight matrix choice. *Nucleic Acids Res.* **22**: 4673–4680.
- Tomkiel, J., Cooke, C.A., Saitoh, H., Bernat, R.L., and Earnshaw, W.C. 1994. CENP-C is required for maintaining proper kinetochore size and for a timely transition to anaphase. *J. Cell Biol.* **125**: 531–545.
- Van Hooser, A.A., Ouspenski, I.I., Gregson, H.C., Starr, D.A., Yen, T.J., Goldberg, M.L., Yokomori, K., Earnshaw, W.C., Sullivan, K.F., and Brinkley, B.R. 2001. Specification of kinetochore-forming chromatin by the histone H3 variant CENP-A. *J. Cell Sci.* **114**: 3529–3542.
- Westermann, S., Cheeseman, I.M., Anderson, S., Yates III, J.R., Drubin, D.G., and Barnes, G. 2003. Architecture of the budding yeast kinetochore reveals a conserved molecular core. *J. Cell Biol.* **163**: 215–222.
- Wigge, P.A. and Kilmartin, J.V. 2001. The Ndc80p complex from *Saccharomyces cerevisiae* contains conserved centromere components and has a function in chromosome segregation. *J. Cell Biol.* **152**: 349–360.
- Yanagawa, S., Lee, J.S., and Ishimoto, A. 1998. Identification and characterization of a novel line of *Drosophila* Schneider S2 cells that respond to wingless signaling. *J. Biol. Chem.* **273**: 32353–32359.
- Yang, C.H., Tomkiel, J., Saitoh, H., Johnson, D.H., and Earnshaw, W.C. 1996. Identification of overlapping DNA-binding and centromere-targeting domains in the human kinetochore protein CENP-C. *Mol. Cell. Biol.* **16**: 3576–3586.